Yang *et al. Applied Biological Chemistry* (2022) 65:67
https://doi.org/10.1186/s13765-022-00735-5

KSABC
The Korean Society for Applied Biological Chemistry

ARTICLE

Open Access

Circ-NT5C2 stimulates FZD4 expression to promote the malignant progression of osteosarcoma by targeting miR-488-3p

Xiaoqi Yang[1], Shuhua Wang[2], Xianjun Zhang[1], Xiangbin Gao[1] and Pengfei Xu[3*]

Abstract

Background: Circ-NT5C2 has been confirmed to be highly expressed and associated to the progression of osteosarcoma (OS). However, the behind mechanism of circ-NT5C2 involvement in OS remains unclear.

Methods: The expression of circ-NT5C2, miR-488-3p and FZD4 was measured by quantitative real-time PCR, and the protein expression of E-cadherin, N-cadherin and FZD4 was detected by western blot. Cell counting kit 8 assay, colony formation assay and 5-ethynyl-2-deoxyuridine assay were performed to assess the cell proliferation. The cell apoptosis was measured by flow cytometry and Caspase3/Caspase9 Activity Assay Kits. Cell migration and invasion were detected by transwell assay. Dual-luciferase reporter assay and RIP assay were carried out to determine the binding relation among circ-NT5C2, miR-488-3p and FZD4. Animal experiment and immunohistochemistry analysis were conducted to explore the role of circ-NT5C2 in tumor growth in vivo.

Results: Comparing with controls, the expression of circ-NT5C2 and FZD4 was upregulated and miR-488-3p expression was downregulated in OS tumor tissues and cells. Circ-NT5C2 overexpression facilitated the cell proliferation and motility and induced cell apoptosis of OS cells, whereas circ-NT5C2 knockdown had the opposite effect. Besides, we also found and confirmed that circ-NT5C2 regulated cell malignant behaviors via modulating miR-488-3p/FZD4 axis in OS. Moreover, circ-NT5C2 silencing repressed the growth of xenografts in vivo.

Conclusion: Circ-NT5C2 upregulated FZD4 expression via sponging miR-488-3p, thus facilitating cell malignant behaviors in OS.

Highlights

1. Circ-NT5C2 is an oncogene in OS.
2. Circ-NT5C2 promotes OS cell malignant behaviors.
3. Circ-NT5C2/miR-488-3p/FZD4 axis is existed in the pathogenesis of OS.

Keywords: Osteosarcoma, Circ-NT5C2, miR-488-3p, FZD4

*Correspondence: yangxiaoqi20211@163.com

[3] Department of Radiotherapy, Affiliated Hospital of Shaanxi University of Traditional Chinese Medicine, No.2, Weiyang West Road, Xianyang 712000, Shaanxi, China
Full list of author information is available at the end of the article

Introduction

Osteosarcoma (OS) originates from mesenchymal cells and occurs mostly in children and adolescents [22, 30]. And it has the characteristics of frequent metastasis, strong invasiveness and high recurrence rate, which usually leads to a poor prognosis [5, 16, 22]. Currently, surgery combined with radiotherapy and chemotherapy is the main treatment strategy for OS therapy [8]. However, the occurrence of chemotherapy resistance greatly limits the effectiveness of OS treatment [18, 21]. Therefore, understanding the pathogenesis of OS, finding specific biomarkers for diagnosis and treatment, and developing safer and more effective treatment strategies is important.

CircRNAs are a new type of non-coding RNA [23]. The ring structure formed by reverse splicing makes the circRNAs structure stable and not easy to be degraded [23]. In addition, circRNAs are widely expressed in multiple species and the sequences are conserved [13]. The above characteristics make circRNAs have the potential to become biomarkers, so circRNAs have attracted the attention of many researchers. As reported, the abnormal expression of circRNAs was related to the pathogenesis of many diseases [4, 10]. CircRNAs could interfere with disease progression by affecting various biological functions such as cell proliferation, metastasis, metabolism and chemotherapy resistance [6, 24, 25]. For example, Huang et al. proved that circ-cESRP1 suppressed TGF-β signal pathway via absorbing miR-93-5p, thereby enhanced the chemosensitivity of small cell lung cancer cells [12]. Besides, studies have revealed that abnormally expressed circRNAs were involved in the process of OS and might be used as biomarkers and therapeutic targets for OS [4, 15]. Circ-NT5C2 (ID: has_circ_0092509), a newly discovered circRNA, has been confirmed to be highly expressed in OS, and was negatively correlated with the patients' survival [20]. However, the specific mechanism of circ-NT5C2 affecting the development of OS has not been studied.

In terms of mechanism, it has been confirmed that circRNAs, as the competitive endogenous RNAs (ceRNAs) of miRNAs, relieved the restriction of miRNAs on the expression of target genes, and thereby affected the cell biological functions [19]. This study confirmed that miR-488-3p was a candidate miRNA for circ-NT5C2 through bioinformatics analysis and related cell experiments. Frizzled homolog 4 (FZD4) is a transmembrane receptor protein, can affect cell function by transducing the Wnt signaling pathway [27]. The TargetScan online software showed that miR-488-3p and FZD4 had targeted binding sites in the sequences. Based on the above information, we hypothesized that circ-NT5C2 might participate in the pathogenesis of OS by regulating the miR-488-3p-mediated FZD4 expression. Therefore, this study firstly investigated the role of circ-NT5C2 in OS, and then further verified the involvement of miR-488-3p/FZD4 axis in the regulation of circ-NT5C2 in OS process.

Materials and methods

Tissue samples

We collected tumor tissues and paired adjacent normal tissues from 47 OS patients from Affiliated Hospital of Jiangnan University. Before conducting this study, we have obtained informed consents and the permission from all patients and the Ethics Committee of Affiliated Hospital of Jiangnan University, respectively.

Cell culture

SW1353, SaOS-2, MG-63 and U2OS cancer cells as well as normal hFOB1.19 cells were brought from ATCC (Manassas, VA, USA). All cells were grown in DMEM (Invitrogen, Carlsbad, CA, USA) plus 10% FBS (Invitrogen) and 1% antibiotics (Invitrogen) with 5% CO^2 at 37 ℃.

Quantitative real-time PCR (qRT-PCR)

PARIS Kit (Invitrogen) was used to obtain the nuclear and cytoplasmic RNAs as per the instructions. After obtaining total RNA by TRIzol Reagent (Invitrogen), Synthesis Kit (Invitrogen) was used to synthesize cDNA, which was mixed with SYBR Green (ABI, Foster City, CA, USA) and specific primers to conduct qRT-PCR. GAPDH and U6 were used to normalize the relative expression of different genes, which were calculated by $2^{-\Delta\Delta Ct}$ method. The utilized primers were listed in Table 1. Three duplicated wells were set for each sample, and three independent biological experiments were conducted.

RNase R assay

The RNA isolated from SW1353 and U2OS cells was treated with or without RNase R (Geneseed, Guangzhou, China), followed by qRT-PCR. Three independent biological experiments were conducted.

Cell transfection

The circ-NT5C2 overexpression plasmid (circ-NT5C2) and siRNAs (si-circ-NT5C2#1 and si-circ-NT5C2#2), the miR-488-3p mimic (miR-488-3p) and miR-488-3p inhibitor (in-miR-488-3p), siRNA of FZD4 (si-FZD4) and the overexpression plasmid of FZD4 (FZD4) and the matching control (Vector, si-con, miR-NC, in-miR-NC, si-NC and pcDNA) were purchased from Genepharma (Shanghai, China) and transfected into SW1353 and U2OS cells.

Table 1 Primers sequences used for PCR

Name		Primers for PCR (5′–3′)
circ-NT5C2	Forward	TGCCAGTCAAGTGATGCGTT
	Reverse	TGGAACTGATGTCTGGACGC
NT5C2	Forward	TACCTACACAGGGCCCCTAC
	Reverse	CCACCCTTGCCGTTTCTTTG
miR-346	Forward	GCCGAGTGTCTGCCCGCAT
	Reverse	CTCAACTGGTGTCGTGGAG
miR-488-3p	Forward	GCCGAGTTGAAAGGCTATT
	Reverse	CTCAACTGGTGTCGTGGAG
miR-593-3p	Forward	GCCGAGTGTCTCTGCTGGG
	Reverse	CTCAACTGGTGTCGTGGAG
miR-654-3p	Forward	GCCGAGTATGTCTGCTGACC
	Reverse	CTCAACTGGTGTCGTGGAG
miR-1182	Forward	GCCGAGGAGGGTCTTGGGAT
	Reverse	CTCAACTGGTGTCGTGGAG
miR-1231	Forward	GCCGAGGTGTCTGGGCGGA
	Reverse	CTCAACTGGTGTCGTGGAG
FZD4	Forward	CAGCAGGACTCAAATGGGGT
	Reverse	CAATGGTTTTCACTGCGGGG
GAPDH	Forward	GACAGTCAGCCGCATCTTCT
	Reverse	GCGCCCAATACGACCAAATC
U6	Forward	CTCGCTTCGGCAGCACA
	Reverse	AACGCTTCACGAATTTGCGT

Cell counting kit 8 (CCK-8) assay

Transfected SW1353 and U2OS cells (1×10^3 cells/well) were grown in 96-well plates and treated with CCK-8 solution (Beyotime, Shanghai, China) at 1, 2, 3, 4, or 5 days for another 4 h. Then, the optical density was detected using a microplate reader at 450 nm. Three duplicated wells were set for each sample, and 3 independent biological experiments were conducted.

Colony formation assay

Transfected SW1353 and U2OS cells were fostered in 6-well plates for 2 weeks. The medium was replaced every 3 days. Subsequently, the cell medium was removed. After fixing and staining the colonies with paraformaldehyde (Beyotime) and crystal violet (Beyotime), the number of colonies were counted under a microscope. Three duplicated wells were set for each sample, and three independent biological experiments were conducted.

5-ethynyl-2-deoxyuridine (EdU) assay

After different transfection, KeyFluor488 EdU Kit (keyGEN Biotech, Jiangsu, China) was employed to measure the DNA synthesis of SW1353 and U2OS cells. After a series of dyeing treatments, the percentage of EdU positive cell (%) was reflected by the number of red signal (EdU positive cells) to blue signal (DAPI positive cells). Three duplicated wells were set for each sample, and three independent biological experiments were conducted.

Cell apoptosis

Transfected SW1353 and U2OS cells were dyed with Annexin V-FITC and PI (Vazyme, Nanjing, China) under the darkness. Then, the apoptotic cells were detected by FACScan flow cytometer. The activity of Caspase3 and Caspase9 was measured using human Cleaved Caspase-3 ELISA Kit (ab220655) or human Caspase-9 ELISA Kit (ab119508) obtained from Abcam (Cambridge, MA, USA) according to instructions. Three independent biological experiments were conducted.

Transwell assay

Matrigel un-coated or coated transwell chambers (Costar, Corning, Switzerland) were used to conduct the transwell migration or invasion assay respectively. After transfection, SW1353 and U2OS cells were resuspended and seeded into the upper chamber. And the bottom chamber was added with medium containing 10% FBS. 24 h later, the number of migrated and invaded cells was counted by a microscope (Leica, Wetzlar, Germany). Three duplicated wells were set for each sample, and 3 independent biological experiments were conducted.

Western blot (WB)

Protein samples were obtained using RIPA buffer (Beyotime). After separating by SDS-PAGE gel, the protein was transferred onto PVDF membranes, and treated with primary antibodies and secondary antibody in turn. The antibodies obtained from Abcam were showed in Table 2. The protein signals were analyzed using Image Lab software. Three independent biological experiments were conducted.

Bioinformatics analysis and dual-luciferase reporter assay

CircBank (http://www.circbank.cn/) and CircInteractome (https://circinteractome.irp.nia.nih.gov/) online software were used to retrieve the candidate miRNAs of circ-NT5C2, and the target of miR-488-3p was predicted by Targetscan online software (http://www.targetscan.org/vert_71/). According to the predicted binding sites, the fragments of wild or mutant circ-NT5C2 and FZD4 3′UTR were cloned into the upstream of pmirGLO luciferase reporter (Promega, Madison, Wisconsin, USA). Afterwards, above reporter vectors and miR-488-3p mimic or the control were transfected into SW1353 and U2OS cells. Dual-Lumi™ II Luciferase Assay Kit (Beyotime) was performed to detect the luciferase activity. Three independent biological experiments were conducted.

Table 2 The antibodies in Western blot

Antibody	Cat	Dilution ratio	Source
E-cadherin	ab40772	1:5000	Abcam
N-cadherin	ab76011	1:5000	Abcam
FZD4	ab277797	1:1000	Abcam
GAPDH	ab181602	1:10000	Abcam
Goat Anti-Rabbit IgG H&L (HRP)	ab6721	1:20000	Abcam

RNA immunoprecipitation (RIP) assay

EZ-Magna RIP kit (Millipore, Billerica, MA, USA) was employed for this assay. Briefly, RIP lysis buffer was used to obtain lysate, which was mixed with RNA magnetic beads coated with Ago2 antibody (Millipore) or IgG antibody (Millipore). Then the enrichment of circ-NT5C2 and miR-488-3p was measured by qRT-PCR. Three independent biological experiments were conducted.

Xenograft model

Male BALB/c nude mice (n = 10) were bought from Charles River Labs (Beijing, China) and randomly divided to 2 group (n = 5/group). Subsequently, sh-circ-NT5C2 or the control sh-con was transfected into U2OS cells, which were subcutaneously injected into the right armpit of each mouse. Tumor volume was measured every week according to the method: Volume (mm^3) = (length × $width^2$)/2. At day 35, all tumors were taken out for other experiments. The animal experiment was approved by the Ethical Committee for Animal Research of Affiliated Hospital of Jiangnan University.

Immunohistochemistry (IHC) assay

Tumor tissues from animals study were used to prepare paraffin sections, which were stained using SP Kit (Invitrogen) and specific antibodies, including anti-FZD4 (1:250, ab277797, Abcam), anti-ki-67 (1:200, ab16667, Abcam) and anti-E-cadherin (1:1000, 20874-1-AP, Proteintech). Three independent biological experiments were conducted.

Statistical analysis

Data were showed as the mean ± standard deviation. Statistical analysis was carried out using GraphPad Prism 8.0 software. Student's *t*-test or one-way ANOVA with Tukey's test were utilized for the comparisons of different groups. The relationship of the levels of circ-NT5C2, miR-488-3p and FZD4 was assayed with Pearson correlation coefficient. Statistical analysis was carried out using GraphPad Prism 8.0 software. $P < 0.05$ was considered as statistically significant.

Results

Circ-NT5C2 is highly expressed in OS tissues and cells

To validate the abnormal expression of circ-NT5C2 in OS, we firstly detected circ-NT5C2 expression in

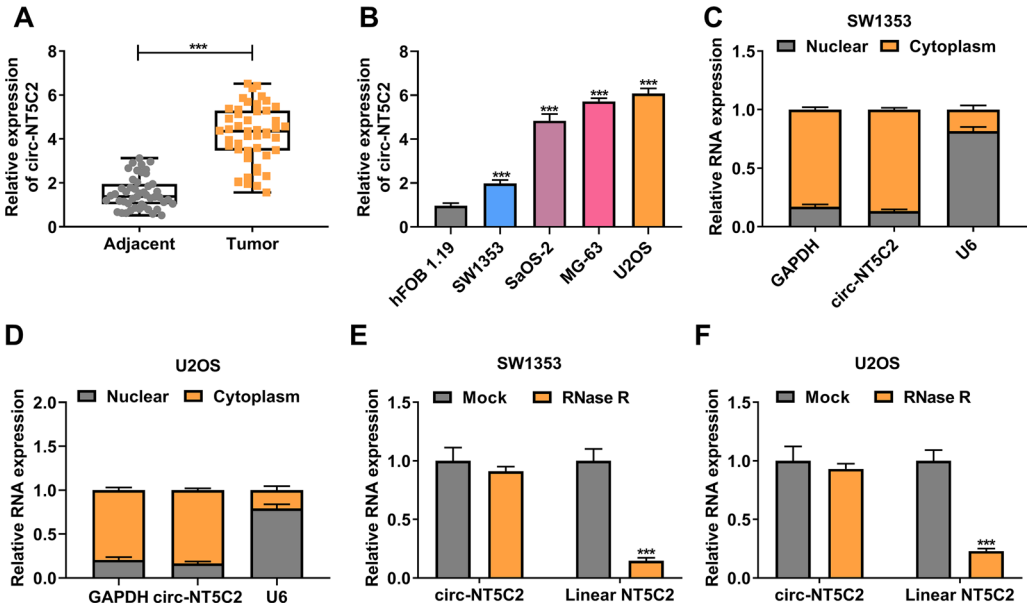

Fig. 1 Circ-NT5C2 was elevated in OS tissues and cells. **A** Circ-NT5C2 expression was measured in 47 paired OS tissues by qRT-PCR. **B** The expression of circ-NT5C2 was detected in hFOB 1.1 and OS cells by qRT-PCR. **C-D** The subcellular localization of circ-NT5C2 was analyzed in SW1353 and U2OS cells. **E**–**F** The circular structure of circ-NT5C2 was confirmed by RNase R assay in SW1353 and U2OS cells. ***$P < 0.001$

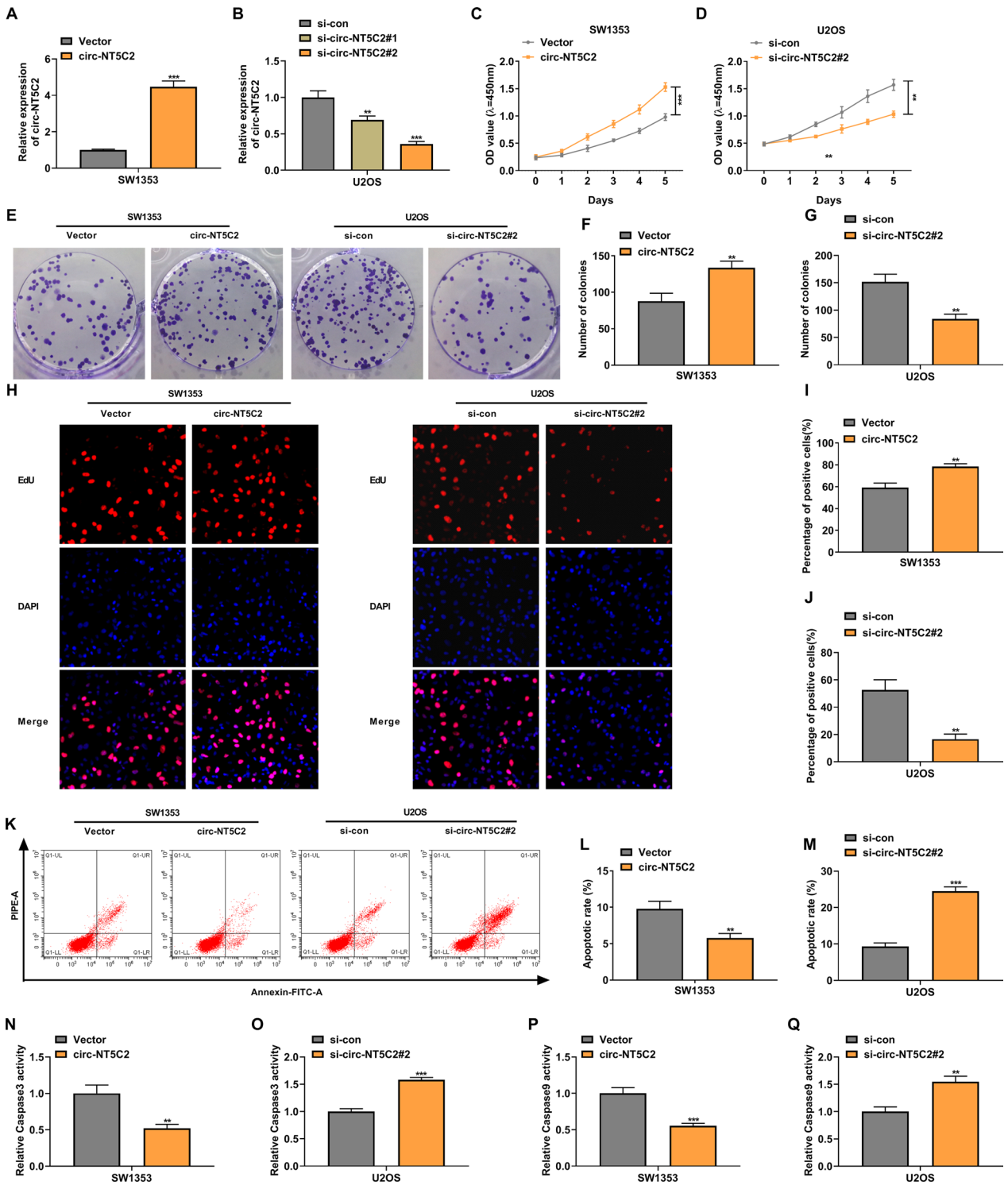

Fig. 2 Circ-NT5C2 facilitated cell proliferation and inhibited cell apoptosis of OS cells. **A**–**B** The overexpression and knockdown transfection efficient of circ-NT5C2 overexpression plasmid and siRNAs was detected by qRT-PCR in SW1353 cells and U2OS cells, respectively. **C**–**Q** SW1353 cells were transfected with Vector or circ-NT5C2, and U2OS cells were transfected with si-con or si-circ-NT5C2#2. **C**–**J** The viability, colony-forming ability and DNA synthesis ability of SW1353 cells and U2OS cells were measured by CCK-8 assay **C**–**D**, colony formation assay **E**–**G** and EdU assay **H**–**J**. **K**–**M** The cell apoptosis of SW1353 cells and U2OS cells was detected by flow cytometry. **N**–**Q** Activity Assay Kits were used to test the Caspase3 and Caspase9 activity. $^{**}P < 0.01$ and $^{***}P < 0.001$

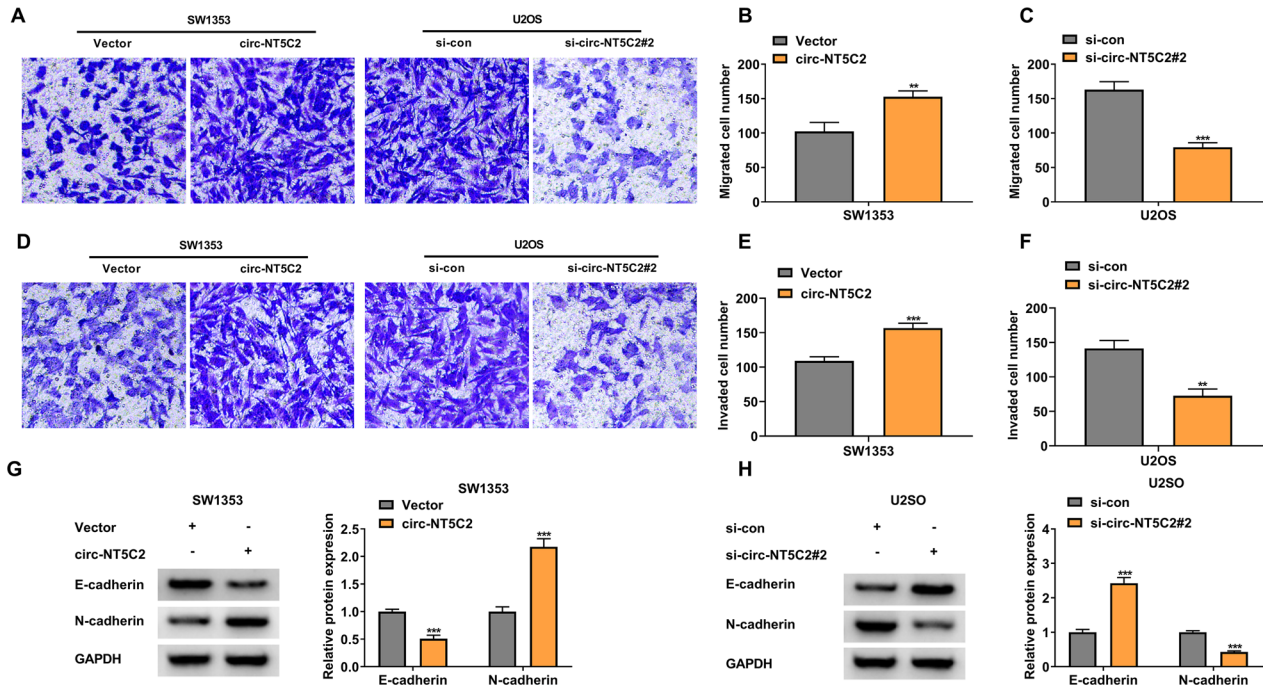

Fig. 3 Circ-NT5C2 promoted OS migration and invasion in vitro. **A**–**H** SW1353 cells were transfected with Vector or circ-NT5C2 and U2OS cells were transfected with si-con or si-circ-NT5C2#2. **A**–**F** The number of migrated and invaded cells was examined by transwell assay. **G**–**H** The protein expression of E-cadherin and N-cadherin was detected by WB. $^{**}P < 0.01$ and $^{***}P < 0.001$

47 paired OS tissues. And the results showed that circ-NT5C2 was overexpressed in OS tumor tissues when comparing to the adjacent normal tissues (Fig. 1A). Next, circ-NT5C2 expression in OS cells was measured and data revealed that circ-NT5C2 was notably upregulated in OS cell lines (SW1353, SaOS-2, MG-63 and U2OS) in comparison with hFOB 1.19 cells (Fig. 1B). In addition, the subcellular localization results presented that circ-NT5C2 was majorly located in the cytoplasm rather than the nucleus of OS cells (Fig. 1C, D), implying that circ-NT5C2 might function as a cytoplasmic miRNA sponge. Subsequently, RNase R assay results uncovered that RNase R treatment sharply downregulated the linear NT5C2 mRNA expression, while circ-NT5C2 expression was lightly affected (Fig. 1E, F). These data indicated that circ-NT5C2 upregulation might be related to OS progression.

Circ-NT5C2 facilitates OS cell proliferation and suppressed OS cell apoptosis in vitro

To investigate the involvement of circ-NT5C2 in OS tumorigenesis, we transfected circ-NT5C2 overexpression plasmid (circ-NT5C2) or siRNAs against circ-NT5C2 (si-circ-NT5C2#1 or si-circ-NT5C2#2) into SW1353 and U2OS cells, resulting in its overexpression or silencing, respectively (Fig. 2A, B; Additional file 1: Fig. S1A, B). Due to the better interference, si-circ-NT5C2#2 was selected for subsequent experiments. Then, CCK-8, colony formation and EdU assay were conducted to assess the proliferation ability of OS cells, and results proved that the viability, colony-forming ability and DNA synthesis ability of SW1353 were promoted by circ-NT5C2 overexpression and circ-NT5C2 knockdown repressed the above effects (Fig. 2C–J; Additional file 1: Fig. S1C–H). Flow cytometry data revealed that overexpressed and silencing circ-NT5C2 restrained or induced the apoptosis of OS cells, respectively (Fig. 2K–M; Additional file 1: Fig. S1I–J). The test results of activity assay kits showed that circ-NT5C2 overexpression suppressed the activity of Caspase3 and Caspase9 in SW1353 cells (Fig. 2N–P; Additional file 1: Fig. S1K–N). On the contrary, circ-NT5C2 silencing enhanced Caspase3 and Caspase9 activity in U2OS cells (Fig. 2O, Q). These findings manifested that circ-NT5C2 promoted cell growth and hindered cell apoptosis in OS cells.

Circ-NT5C2 contributes to OS motility in vitro

Next, we further explored the influence of circ-NT5C2 in OS cell motility using transwell assay,

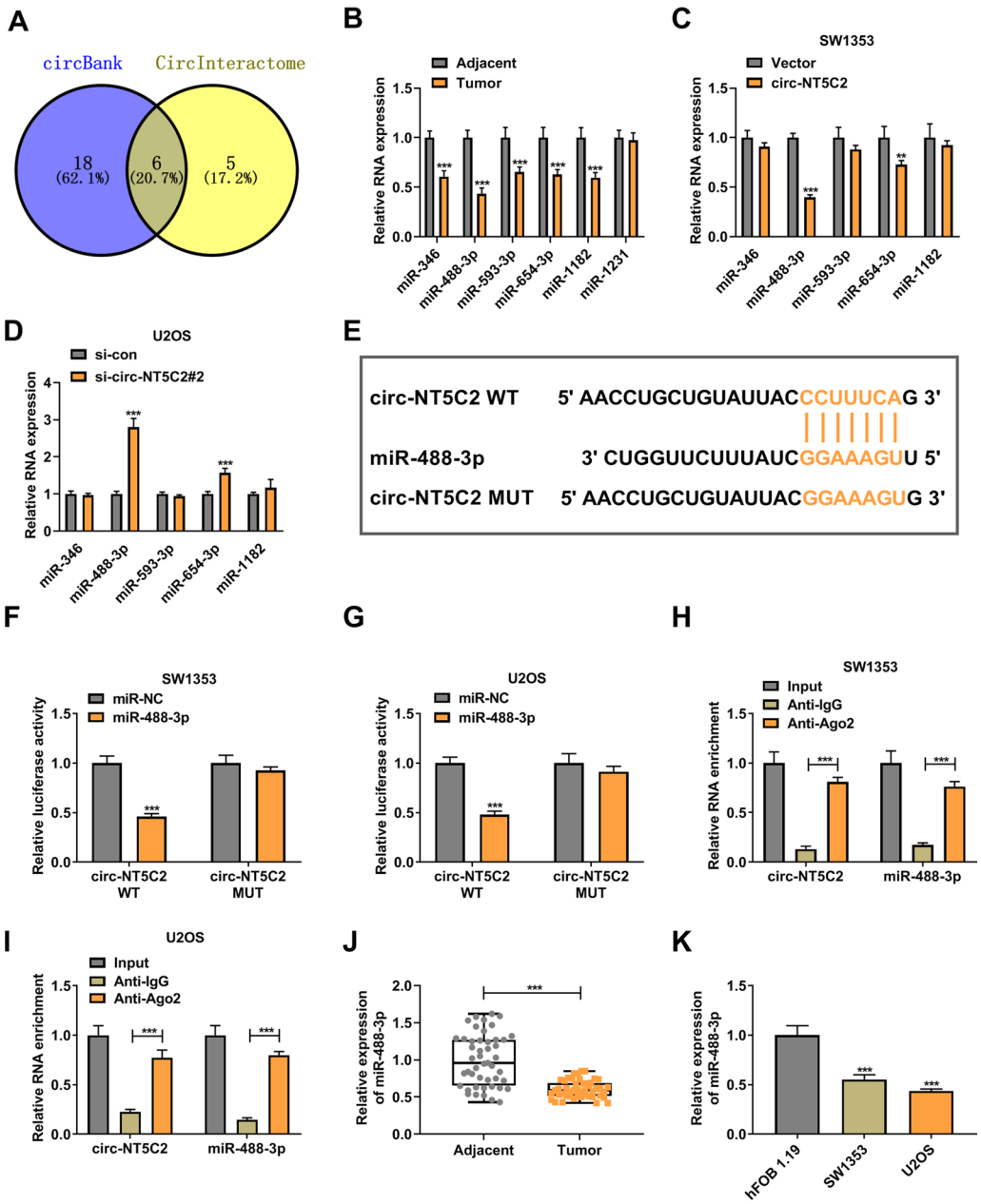

Fig. 4 Circ-NT5C2 was physically interacted with miR-488-3p via target binding. **A** The number of miRNAs that were predicted as targets for circ-NT5C2 in circBank and CircInteractome online software was showed in Venn diagram. **B** The expression of miR-346, miR-488-3p, miR-593-3p, miR-654-3p, miR-1182 and miR-1231 was measured by qRT-PCR in 6 pairs of OS tissues randomly selected. **C**–**D** The expression of miR-346, miR-488-3p, miR-593-3p, miR-654-3p and miR-1182 was determined by qRT-PCR in SW1353 cells transfected with Vector or circ-NT5C2, and U2OS cells transfected with si-con or si-circ-NT5C2#2. **E** The binding sites of miR-488-3p and circ-NT5C2 WT or MUT Vector were showed. **F**–**G** Dual-luciferase reporter assay was performed to determine the luciferase activity in SW1353 cells and U2OS cell transfected with circ-NT5C2 WT/MUT reporter vector and miR-488-3p or miR-NC. **H**–**I** RIP assay and qRT-PCR were conducted to detect the enrichment of circ-NT5C2 and miR-488-3p. **J**–**K** The expression of circ-NT5C2 was measured by qRT-PCR in 47 pairs of OS tissues as well as hFOB 1.19, SW1353 cells and U2OS cells. $^{**}P < 0.01$ and $^{***}P < 0.001$

and data showed that circ-NT5C2 overexpression increased the migrated and invaded number of SW1353 cells, whereas circ-NT5C2 knockdown suppressed the migration and invasion abilities of U2OS cells (Fig. 3A–F). In support, the related markers of cell metastasis (E-cadherin and N-cadherin) were detected by WB analysis. The results revealed that the expression of E-cadherin was reduced and the N-cadherin expression was increased after transfecting circ-NT5C2 overexpression plasmid into SW1353 cells. On the contrary, circ-NT5C2 silencing upregulated E-cadherin expression and downregulated N-cadherin expression (Fig. 3G, H). These outcomes displayed that circ-NT5C2 reinforced the abilities of cell migration and invasion in OS cells.

Circ-NT5C2 interacts with miR-488-3p

A total of six miRNAs were predicted to harbor binding sites with circ-NT5C2, which was predicted in both circBank and CircInteractome online software (Fig. 4A). Comparing with adjacent tissues, 5 miRNAs (miR-346, miR-488-3p, miR-593-5p, miR-654-3p and miR-1182) expression was significantly downregulated in 6 pairs of OS tumor tissues randomly selected (Fig. 4B). Then, we detected the expression of the 5 miRNAs mentioned above after circ-NT5C2 overexpression or silencing, data revealed that only 2 miRNAs including miR-488-3p and miR-654-3p were regulated by circ-NT5C2 in OS cells (Fig. 4C, D). Considering that response of miR-488-3p to circ-NT5C2 was more significant, miR-488-3p was selected for subsequent analysis. The binding sites of miR-488-3p and WT or MUT circ-NT5C2 were showed in Fig. 4E. To further verify this target relationship, the WT or MUT circ-NT5C2 reporter vector and miR-NC or miR-488-3p were transfected into SW1353 and U2OS cells, and the luciferase activity of circ-NT5C2 WT reporter vector rather than circ-NT5C2 MUT reporter vector was notably decreased by miR-488-3p overexpression (Fig. 4F, G). RIP assay results displayed that the enrichment of circ-NT5C2 and miR-488-3p on Ago2 was higher than that on IgG (Fig. 4H, I). Additionally, the low expression of miR-488-3p was appeared in OS tumor tissues and cells in contrast to the controls (Fig. 4J, K). Taken together, the above results indicated that circ-NT5C2 acted as a sponge of miR-488-3p in OS.

Circ-NT5C2 promotes OS cell malignant behaviors in vitro via sponging miR-488-3p

Subsequently, whether miR-488-3p was involved in the action of circ-NT5C2 in OS cells was investigated. After confirming the overexpression efficiency of miR-488-3p mimic in SW1353 cells and knockdown efficiency of miR-488-3p inhibitor in U2OS cells (Fig. 5A, B), miR-488-3p mimic or inhibitor were respectively transfected into circ-NT5C2-overexpressed SW1353 cells or circ-NT5C2-silenced U2OS cells to conduct rescue experiments. CCK-8, colony formation and EdU assay results showed that miR-488-3p mimic relieved the proliferation-promoting effect induced by circ-NT5C2 overexpression in SW1353 cells, while miR-488-3p inhibitor could restore the proliferation-suppressing effect mediated by circ-NT5C2 knockdown in U2OS cells (Fig. 5C–H). Flow cytometry and activity assay kits displayed that miR-488-3p mimic abolished circ-NT5C2 overexpression-induced inhibition of the cell apoptosis in SW1353 cells, and circ-NT5C2 silencing-mediated promotion of U2OS cell apoptosis was overturned by miR-488-3p inhibitor (Fig. 5I–L). In addition, the promotion mediated by overexpressed circ-NT5C2 in the cell migration and invasion of SW1353 cells was rescued after co-transfecting with miR-488-3p mimic, and miR-488-3p inhibitor could restore the suppressive impacts of circ-NT5C2 silencing in U2OS cell migration and invasion (Fig. 5M–P). Moreover, miR-488-3p overexpression relieved the downregulation of E-cadherin expression and the upregulation of N-cadherin mediated by circ-NT5C2 overexpression. On the contrary, circ-NT5C2 knockdown induced E-cadherin expression and repressed N-cadherin expression, and these effects were attenuated by co-transfecting with miR-488-3p inhibitor (Fig. 5Q, R). These rescue experiments results confirmed that circ-NT5C2 contributed to the malignant phenotypes of OS cells via sponging miR-488-3p.

FZD4 acts as a miR-488-3p target

FZD4 was a possible target gene of miR-488-3p according to the predicted result of TargetScan online software, and the binding sites were showed in Fig. 6A. To investigate the influence of miR-488-3p on FZD4 expression, we transfected miR-488-3p mimic and inhibitor

(See figure on next page.)

Fig. 5 The regulation of circ-NT5C2 on OS cells malignant behaviors in vitro was relieved by miR-497-5p. **A–B** The overexpression and knockdown transfection efficient of miR-488-3p mimic and inhibitor was confirmed by qRT-PCR in SW1353 cells and U2OS cells, respectively. **C–R** SW1353 cells were transfected with Vector, circ-NT5C2, circ-NT5C2 + miR-NC, circ-NT5C2 + miR-488-3p and U2OS were transfected with si-NC, si-circ-NT5C2#2, si-circ-NT5C2#2 + in-miR-NC, or si-circ-NT5C2#2 + in-miR-488-3p. **C–H** The cell proliferation was assessed by CCK-8 assay **C–D**, colony formation assay **E–F** and EdU assay (**G–H**). **I–J** The cell apoptosis of was detected by flow cytometry. **K–L** Activity Assay Kits were used to test the Caspase3 and Caspase9 activity. **M–P** The cell migration and invasion were determined by transwell assay. **Q–R** The protein expression of E-cadherin and N-cadherin was detected by WB. $^{*}P < 0.05$, $^{**}P < 0.01$ and $^{***}P < 0.001$

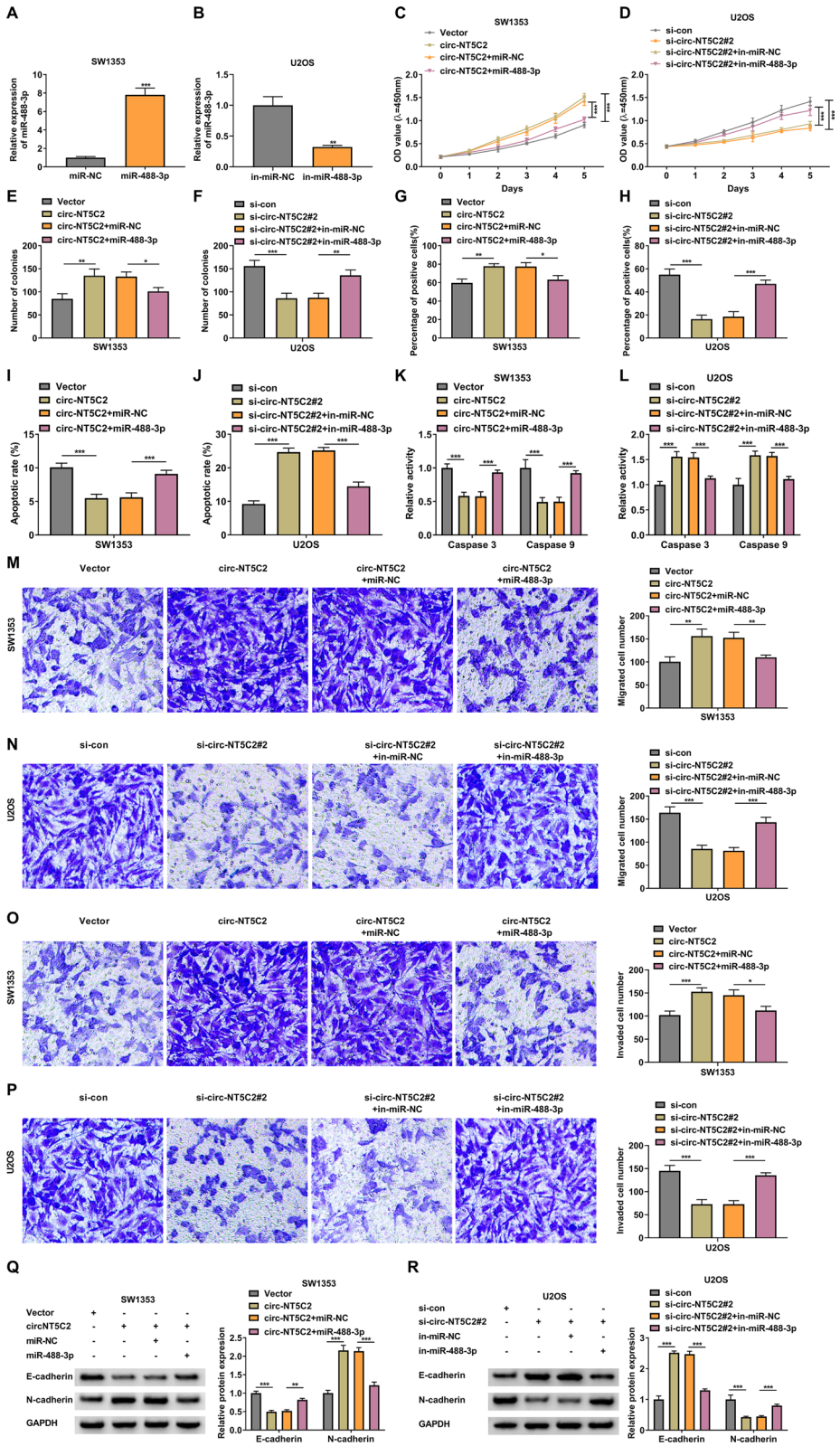

Fig. 5 (See legend on previous page.)

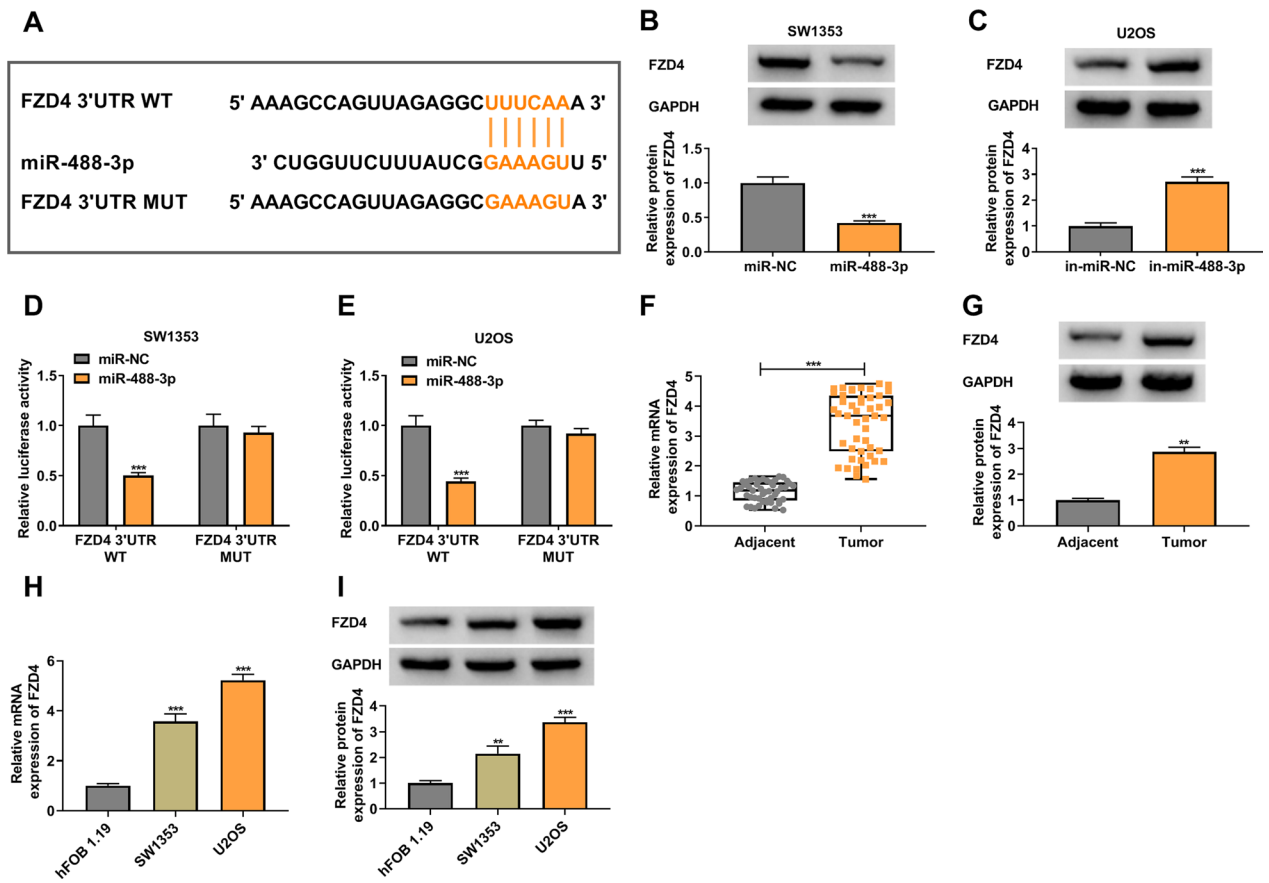

Fig. 6 MiR-488-3p directly targeted FZD4. **A** The binding sites of miR-488-3p and FZD4 3'UTR MT and MUT vector were predicted by TargetScan online software. **B–C** FZD4 expression was detected by WB in SW1353 cells transfected with miR-NC or miR-488-3p and U2OS cells transfected with in-miR-NC or in-miR-488-3p. **D–E** The luciferase activity was measured by dual-luciferase reporter assay in SW1353 and U2OS cells transfected with FZD4 3'UTR WT/MUT reporter vector and miR-488-3p or miR-NC. **F–I** FZD4 expression was examined by qRT-PCR and WB in OS tissues and cell samples. $^{**}P < 0.01$ and $^{***}P < 0.001$

into SW1353 and U2OS cells, respectively. WB results revealed that miR-488-3p mimic downregulated the protein expression of FZD4 in SW1353 cells, whereas miR-488-3p inhibitor upregulated FZD4 protein expression in U2OS cells (Fig. 6B, C). Besides, the dual-luciferase reporter assay data showed that miR-488-3p remarkably decreased the luciferase activity of FZD4 3'UTR WT reporter vector, but had no influence on the luciferase activity of FZD4 3'UTR MUT reporter vector (Fig. 6D, E). Then, qRT-PCR and WB were performed to detect the mRNA and protein expression of FZD4 in OS tissues and cells. Comparing to adjacent normal tissues and hFOB 1.19 cells, the higher level of FZD4 mRNA and protein was appeared in OS tumor tissues and cells (Fig. 6F–I). These data suggested that FZD4 was a target gene of miR-488-3p.

(See figure on next page.)

Fig. 7 MiR-488-3p regulated OS cell functions via targeting FZD4. **A** The knockdown and overexpression transfection efficiency of miR-488-3p inhibitor and mimic was separately confirmed by qRT-PCR in SW1353 cells and U2OS cells. **B** The knockdown and overexpression transfection efficiency of si-FZD4 and FZD4 overexpression plasmid was verified by WB in SW1353 cells and U2OS cells. **C–R** in-miR-NC, in-miR-488-3p, in-miR-488-3p + si-NC or in-miR-488-3p + si-FZD4 was transfected into SW1353 cells, while miR-NC, miR-488-3p, miR-488-3p + pcDNA or miR-488-3p + FZD4 was transfected into U2OS cells. **C–H** CCK-8 assay **C**, **D**, colony formation assay **E–F** and EdU assay **G–H** were performed to detect the cell proliferation. **I–J** The cell apoptosis was detected by flow cytometry. **K–L** Activity Assay Kits were used to test the Caspase3 and Caspase9 activity. **M–P** The migrated and invaded cells was measured by transwell assay. **Q–R** The protein expression of E-cadherin and N-cadherin was detected by WB. $^{**}P < 0.01$ and $^{***}P < 0.001$

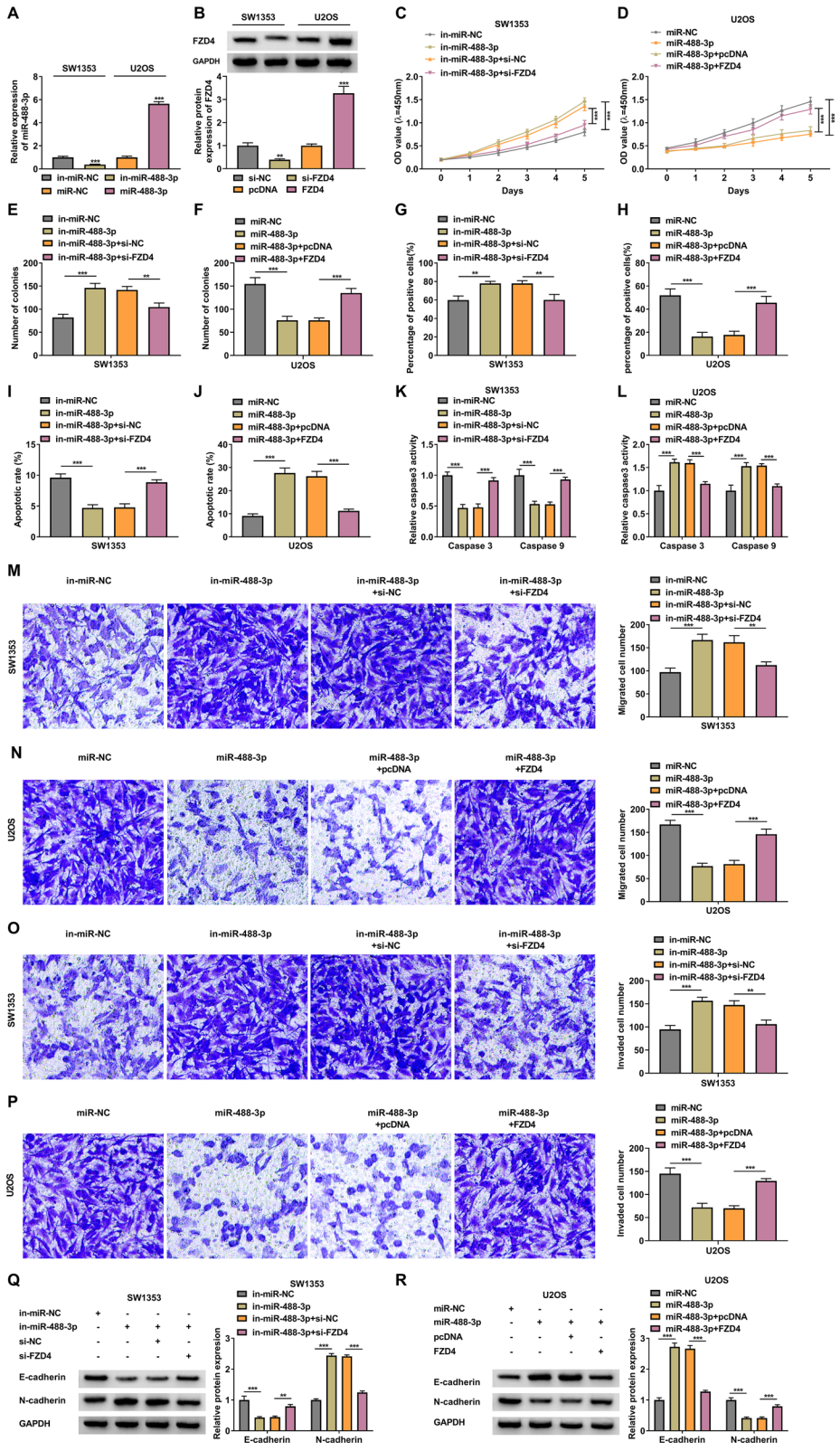

Fig. 7 (See legend on previous page.)

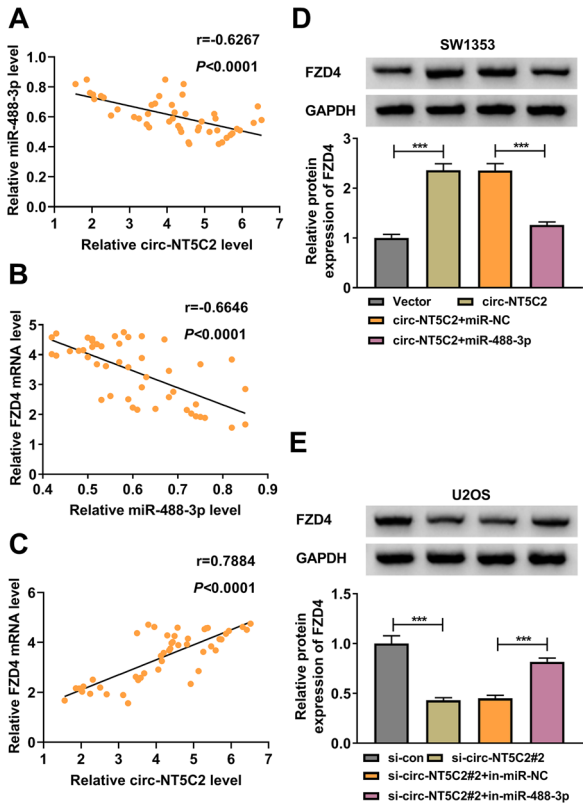

Fig. 8 Circ-NT5C2 upregulated FZD4 expression via sponging miR-488-3p. **A**–**C** The linear correlation between the levels of circ-NT5C2, miR-488-3p and FZD4 in OS tissues was analyzed using Pearson correlation coefficient. **D**–**E** FZD4 protein expression was detected by WB in SW1353 cells transfected with vector, circ-NT5C2, circ-NT5C2 + miR-NC, or circ-NT5C2 + miR-488-3p and U2OS cells transfected with si-NC, si-circ-NT5C2#2, si-circ-NT5C2#2 + in-miR-NC, or si-circ-NT5C2#2 + in-miR-488-3p. ***$P < 0.001$

MiR-488-3p suppresses OS cell malignant behaviors in vitro via targeting FZD4

Subsequently, the functionality of FZD4 was explored in OS cells. The findings exhibited that FZD4 absence restrained cell proliferative ability and colony-forming ability, reduced the number of EdU-positive cells, strengthened cell apoptosis rate, and repressed cell migratory and invasive abilities; as expected, FZD4 overexpression showed the opposite effects (Additional file 2: Fig. S2A–L). Considering the above findings, rescue experiments were performed to validate the role of miR-488-3p and FZD4 in OS progression. First, we confirmed the knockdown and overexpression efficient of miR-488-3p inhibitor and mimic in SW1353 cells and U2OS cells, respectively (Fig. 7A). Then, si-FZD4 and FZD4 overexpression plasmid were separately transfected into SW1353 and U2OS cells to downregulate and upregulated FZD4 expression (Fig. 7B). Subsequently, we performed CCK-8, colony formation and EdU assay to assess the proliferation of OS cells. MiR-488-3p inhibitor notably facilitated the viability, colony-forming ability and DNA synthesis ability of SW1353 cells, FZD4 knockdown co-transfecting could revert these proliferation-promoting effects (Fig. 7C, E, G). Besides, FZD4 overexpression attenuated the proliferation-suppressing effects of miR-488-3p mimic in U2OS cells (Fig. 7D, F, H). Apoptosis related experiments showed that the inhibition of cell apoptosis mediated by miR-488-3p knockdown in SW1353 cells was relieved by FZD4 silencing, while overexpressed FZD4 restored the promotion of U2OS cell apoptosis induced by miR-488-3p overexpression (Fig. 7I–L). Additionally, miR-488-3p inhibitor significantly induced cell migration and invasion, and these impacts were overturned by FZD4 knockdown in SW1353 cells (Fig. 7M, O). On the contrary, miR-488-3p mimic suppressed U2OS cell migration and invasion, whereas overexpressed FZD4 could rescue the above effects (Fig. 7N, P). Moreover, WB results showed that FZD4 silencing reverted the downregulation of E-cadherin expression and the upregulation of N-cadherin expression mediated by miR-488-3p inhibitor, while FZD4 overexpression restored the regulation of miR-488-3p mimic on the expression of E-cadherin and N-cadherin (Fig. 7Q, R). All these data illustrated that miR-488-3p regulated the malignant behaviors of OS cells by targeting FZD4.

Circ-NT5C2 indirectly promotes FZD4 expressionvia absorbing miR-488-3p

In OS tumor tissues, we found that there was a negatively correlation between circ-NT5C2 and miR-488-3p expression (Fig. 8A). Besides, the level of FZD4 mRNA was negatively correlated with miR-488-3p level and positively correlated with circ-NT5C2 level in OS tumor tissues (Fig. 8B, C). Moreover, we discovered that circ-NT5C2 overexpression notably promoted the expression of FZD4 protein, and this effect was reverted by miR-488-3p mimic (Fig. 8D). And miR-488-3p inhibitor restored the suppressive effect of FZD4 expression mediated by circ-NT5C2 knockdown (Fig. 8E). These findings indicated that circ-NT5C2 positively regulated FZD4 expression via sponging miR-488-3p.

Silencing of circ-NT5C2 represses OS tumor growth in vivo

To further explore the effect of circ-NT5C2 in OS tumor growth, U2OS cells transfected with sh-con or sh-circ-NT5C2 were injected into nude mice to construct xenograft mice model. Five weeks later, tumor volume and weight in sh-circ-NT5C2 group were smaller than that in sh-NC group (Fig. 9A–C). Comparing to the sh-NC group, circ-NT5C2 and FZD4 expression were downregulated, while miR-488-3p expression was upregulated in the tumor tissues of sh-NT5C2 group (Fig. 9D–F). Besides, circ-NT5C2 knockdown facilitated

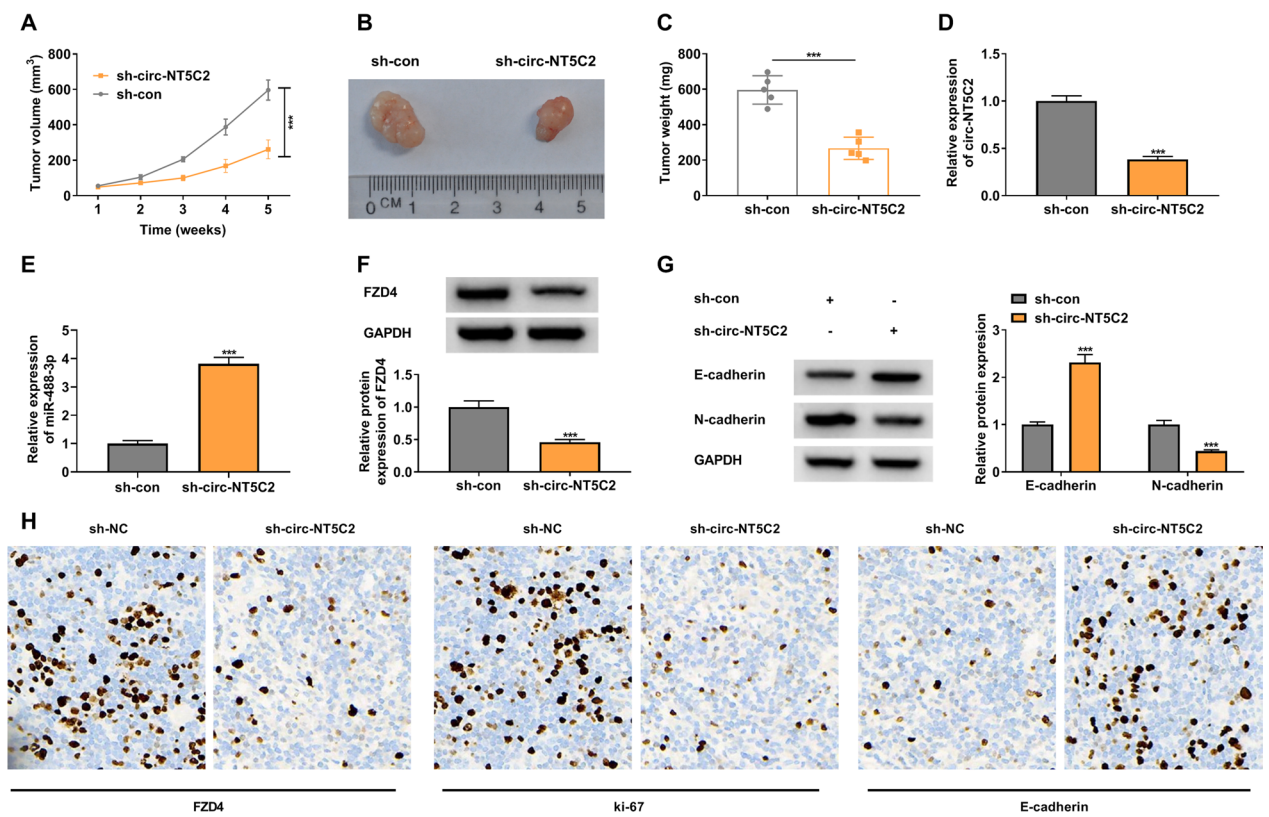

Fig. 9 Circ-NT5C2 depletion restrained OS tumorigenesis. **A**–**C** The representative images, growth curve and weight of xenografts was showed. **D**–**E** The expression of circ-NT5C2 **D** and miR-497-5p **E** was determined by qRT-PCR. **F**–**G** WB was performed to detect the protein expression of FZD4 **F**, E-cadherin and N-cadherin **G**. **H** IHC assay was conducted to stain the positive cells of FZD4, ki-67 and E-cadherin. ***$P < 0.001$

the expression of E-cadherin and suppressed N-cadherin expression (Fig. 9G). Moreover, IHC assay results showed that the positive cells of FZD4 and ki-67 were decreased, while the positive cells of E-cadherin were increased in the tumor tissues of sh-circ-NT5C2 group (Fig. 9H). In general, the above data demonstrated that circ-NT5C2 was a pro-tumor factor in OS.

Discussion

OS is a major threat to human health due to the high mortality and morbidity [16]. Although researchers have been working to improve therapy, the ontcomes of OS patients remain poor [8]. Thus, finding possible therapeutic targets to improve the current status of OS treatment t is urgent. This study found that circ-NT5C2, a novel circRNA overexpressed in OS, participated in modulating the biological functions of OS cells. Additionally, we discovered and confirmed the molecular mechanism of circ-NT5C2 in OS.

Recent studies have shown that circRNAs were involved in the progress of OS. For instance, Cao et al. proved that circ_0008932 facilitated OS cells proliferation and motility via absorbing miR-145-5p [2]. Gao et al. confirmed that suppression of circ_0084582 restrained the malignant phenotypes of OS cells via sponging miR-485-3p and thereby regulating JAG1 expression [7]. In another study, Guan et al. found that highly expressed circ_0001721 contributed to TCF4 expression, cell growth and metastasis in doxorubicin-resistant OS cells by targeting miR-758 [9]. Although studies have confirmed that high level of circ-NT5C2 appeared in OS tumor tissues through RNA sequencing, there was no research on the specific role and mechanism of circ-NT5C2 in the pathogenesis of OS [20]. Here, we confirmed that circ-NT5C2 was overexpressed in OS tumor tissues. In addition, overexpression or knockdown of circ-NT5C2 promoted or inhibited the malignant behaviors of OS cells, respectively. In vivo experiments further confirmed that circ-NT5C2 was a promoting factor in the development of OS.

Accumulated research data showed that miRNAs were important regulators in cancer progression by regulating cell functions in various cancers, including OS [11, 14]. In addition, studies have analyzed the expression of miRNAs in OS plasma samples in the Gene Expression Comprehensive database and found that the expression of miRNAs in OS patients was abnormally expressed when

comparing with the controls [26]. This study found and confirmed that miR-488-3p was targeted by circ-NT5C2. MiR-488-3p, as a tumor suppressor, has been reported that it was closely related to the development of colorectal cancer [17], papillary thyroid cancer [31] and esophageal squamous cell carcinoma [28]. It was worth noting that Bu et al. found that lncRNA SNHG16 promoted the progression of OS through negative regulation of miR-488-3p [1]. Here, the rescue experiments further verified that circ-NT5C2 regulated the function of OS cells through targeting miR-488-3p.

FZDs, a type of G protein-coupled receptors, have been shown to have significant roles in Wnt signal transduction [27]. FZD4 is a member of the FZDs. As reported, FZD4 was an oncogene and significantly upregulated in many cancers [3, 29, 32]. For example, FZD4 was promoted by circ_0004712/miR-331-3p axis in the progression of ovarian cancer [32]. MiR-101 restrained FZD4 expression and thereby suppressing the motility of bladder cancer cells [3]. Besides, lncRNA SNHG1 contributed to FZD4 expression, and attenuated the anti-cancer effect of baicalein via sponging miR-3127-5p [29]. This study firstly discovered an upregulated FZD4 in OS. Additionally, FZD4 silencing restored the promotion of miR-488-3p inhibitor on OS cells proliferation and metastasis, while overexpressed FZD4 relieved the inhibition of 488-3p mimic on the cell growth and metastasis of OS cells, implying that miR-488-3p/FZD4 axis was existed in the process of OS.

In conclusion, our research confirmed that as a new ceRNA axis, the circ-NT5C2/miR-488-3p/FZD4 axis affected the malignant progression of OS by regulating cell growth, motility and apoptosis of OS cells. These findings provided basic support for revealing the internal mechanism and developing therapeutic strategy of OS.

Supplementary Information

The online version contains supplementary material available at https://doi.org/10.1186/s13765-022-00735-5.

Additional file 1: Fig. S1 Circ-NT5C2 facilitated cell proliferation, migration and invasion, and inhibited cell apoptosis of OS cells. (A–B) The overexpression and knockdown transfection efficient of circ-NT5C2 overexpression plasmid and siRNAs was detected by qRT-PCR. (C–N) U2OS cells were transfected with Vector or circ-NT5C2, and SW1353 cells were transfected with si-con or si-circ-NT5C2#2. (C–H) The viability, colony-forming ability and DNA synthesis ability of SW1353 cells and U2OS cells were measured by CCK-8 assay (C–D), colony formation assay (E–F) and EdU assay (G–H). (I–J) The cell apoptosis of SW1353 cells and U2OS cells was detected by flow cytometry. (K–N) The number of migrated and invaded cells was examined by transwell assay. *P<0.05, **P<0.01 and ***P<0.001.

Additional file 2: Fig. S2 FZD4 elevation aggravated OS cell malignant phenotypes. (A–B) The effects of FZD4 knockdown and overexpression on cell proliferation were evaluated by CCK-8 assay. (C–D) The effects of FZD4 knockdown and overexpression on colony-forming ability were evaluated by colony formation assay. (E–F) The effects of FZD4 knockdown and overexpression on DNA synthesis were evaluated by EdU assay. (G–H) The effects of FZD4 knockdown and overexpression on cell apoptosis were checked by flow cytometry assay. (I–L) The effects of FZD4 knockdown and overexpression on cell migration and invasion were examined by transwell assay. **P<0.01 and ***P<0.001.

Acknowledgements
Not applicable.

Author contributions
All authors made substantial contribution to conception and design, acquisition of the data, or analysis and interpretation of the data; take part in drafting the article or revising it critically for important intellectual content; gave final approval of the revision to be published; and agree to be accountable for all aspect of the work. All authors read and approved the final manuscript.

Funding
This study was supported by The Key Funding Projects for Independent Innovation of Health System Research in Putuo District, Shanghai (Grant No. SH201741).

Availability of data and materials
The analyzed data sets generated during the present study are available from the corresponding author on reasonable request.

Declarations

Ethics approval and consent to participate
The present study was approved by the ethical review committee of Affiliated Hospital of Jiangnan University. Written informed consent was obtained from all enrolled patients.

Consent for publication
Not applicable.

Competing interests
The authors declare that they have no competing interests.

Author details
[1]Department of Orthopaedics, Affiliated Hospital of Jiangnan University, Wuxi 214035, Jiangsu, China. [2]Department of Orthopedics, Xingguo People's Hospital of Jiangxi Province, Ganzhou 342400, Jiangxi, China. [3]Department of Radiotherapy, Affiliated Hospital of Shaanxi University of Traditional Chinese Medicine, No.2, Weiyang West Road, Xianyang 712000, Shaanxi, China.

Received: 23 May 2022 Accepted: 4 October 2022
Published online: 31 October 2022

References

1. Bu J, Guo R, Xu XZ, Luo Y, Liu JF (2021) LncRNA SNHG16 promotes epithelial-mesenchymal transition by upregulating ITGA6 through miR-488 inhibition in osteosarcoma. J Bone Oncol 27:100348. https://doi.org/10.1016/j.jbo.2021.100348
2. Cao C, Shu X (2021) Suppression of circ_0008932 inhibits tumor growth and metastasis in osteosarcoma by targeting miR-145-5p. Exp Ther Med 22(4):1106. https://doi.org/10.3892/etm.2021.10540
3. Chen L, Long Y, Han Z, Yuan Z, Liu W, Yang F, Li T, Shu L, Zhong Y (2019) MicroRNA-101 inhibits cell migration and invasion in bladder cancer via targeting FZD4. Exp Ther Med 17(2):1476–1485. https://doi.org/10.3892/etm.2018.7084
4. Chen W, Zhang B, Chang X (2021) Emerging roles of circular RNAs in osteoporosis. J Cell Mol Med. https://doi.org/10.1111/jcmm.16906
5. Chong ZX, Yeap SK, Ho WY (2021) Unraveling the roles of miRNAs in regulating epithelial-to-mesenchymal transition (EMT) in osteosarcoma. Pharmacol Res 172:105818. https://doi.org/10.1016/j.phrs.2021.105818

6. Dong H, Zhou J, Cheng Y, Wang M, Wang S, Xu H (2021) Biogenesis, functions, and role of circrnas in lung cancer. Cancer Manag Res 13:6651–6671. https://doi.org/10.2147/CMAR.S324812
7. Gao P, Zhao X, Yu K, Zhu Z (2021) Circ_0084582 facilitates cell growth, migration, invasion, and angiopoiesis in osteosarcoma via mediating the mir-485–3p/JAG1 axis. Front Genet 12:690956. https://doi.org/10.3389/fgene.2021.690956
8. Gill J, Gorlick R (2021) Advancing therapy for osteosarcoma. Nat Rev Clin Oncol. https://doi.org/10.1038/s41571-021-00519-8
9. Guan H, Xu H, Chen J, Wu W, Chen D, Chen Y, Sun J (2021) Circ_0001721 enhances doxorubicin resistance and promotes tumorigenesis in osteosarcoma through miR-758/TCF4 axis. Cancer Cell Int 21(1):336. https://doi.org/10.1186/s12935-021-02016-5
10. Harper KL, Mottram TJ, Whitehouse A (2021) Insights into the evolving roles of circular RNAs in cancer. Cancers 13:16. https://doi.org/10.3390/cancers13164180
11. Hosseini F, Alemi F, Malakoti F, Mahmoodpoor A, Younesi S, Yousefi B, Asemi Z (2021) Targeting Wnt/beta-catenin signaling by microRNAs as a therapeutic approach in chemoresistant osteosarcoma. Biochem Pharmacol 193:114758. https://doi.org/10.1016/j.bcp.2021.114758
12. Huang W, Yang Y, Wu J, Niu Y, Yao Y, Zhang J, Huang X, Liang S, Chen R, Chen S et al (2020) Circular RNA cESRP1 sensitises small cell lung cancer cells to chemotherapy by sponging miR-93-5p to inhibit TGF-beta signalling. Cell Death Differ 27(5):1709–1727. https://doi.org/10.1038/s41418-019-0455-x
13. Kristensen LS, Andersen MS, Stagsted LVW, Ebbesen KK, Hansen TB, Kjems J (2019) The biogenesis, biology and characterization of circular RNAs. Nat Rev Genet 20(11):675–691. https://doi.org/10.1038/s41576-019-0158-7
14. Li B, Cao Y, Sun M, Feng H (2021) Expression, regulation, and function of exosome-derived miRNAs in cancer progression and therapy. FASEB J 35(10):e21916. https://doi.org/10.1096/fj.202100294RR
15. Li Z, Li X, Xu D, Chen X, Li S, Zhang L, Chan MTV, Wu WKK (2021) An update on the roles of circular RNAs in osteosarcoma. Cell Prolif 54(1):e12936. https://doi.org/10.1111/cpr.12936
16. Lindsey BA, Markel JE, Kleinerman ES (2017) Osteosarcoma overview. Rheumatol Ther 4(1):25–43. https://doi.org/10.1007/s40744-016-0050-2
17. Liu Y, Peng H, Shen Y, Da R, Tian A, Guo X (2020) Downregulation of long noncoding rna myocardial infarction associated transcript suppresses cell proliferation, migration, invasion, and glycolysis by regulation of mir-488-3p/IGF1R pathway in colorectal cancer. Cancer Biother Radiopharm. https://doi.org/10.1089/cbr.2020.3671
18. Marchandet L, Lallier M, Charrier C, Baud'huin M, Ory B, Lamoureux F (2021) Mechanisms of Resistance to conventional therapies for osteosarcoma. Cancers 13:4. https://doi.org/10.3390/cancers13040683
19. Min X, Liu DL, Xiong XD (2021) Circular RNAs as competing endogenous RNAs in cardiovascular and cerebrovascular diseases: molecular mechanisms and clinical implications. Front Cardiovasc Med 8:682357. https://doi.org/10.3389/fcvm.2021.682357
20. Nie WB, Zhao LM, Guo R, Wang MX, Ye FG (2021) Circular RNA circ-NT5C2 acts as a potential novel biomarker for prognosis of osteosarcoma. Eur Rev Med Pharmacol Sci. 25(5):2154. https://doi.org/10.2635/eurrev_202103_25193
21. Prudowsky ZD, Yustein JT (2020) Recent insights into therapy resistance in osteosarcoma. Cancers 13:1. https://doi.org/10.3390/cancers13010083
22. Rathore R, Van Tine BA (2021) Pathogenesis and current treatment of osteosarcoma: perspectives for future therapies. J Clin Med 10:6. https://doi.org/10.3390/jcm10061182
23. Tao M, Zheng M, Xu Y, Ma S, Zhang W, Ju S (2021) CircRNAs and their regulatory roles in cancers. Mol Med 27(1):94. https://doi.org/10.1186/s10020-021-00359-3
24. Xin C, Huang F, Wang J, Li J, Chen Q (2021) Roles of circRNAs in cancer chemoresistance (Review). Oncol Rep 46:4. https://doi.org/10.3892/or.2021.8176
25. Xing Z, Wang R, Wang X, Liu J, Zhang M, Feng K, Wang X (2021) CircRNA circ-PDCD11 promotes triple–negative breast cancer progression via enhancing aerobic glycolysis. Cell Death Discov 7(1):218. https://doi.org/10.1038/s41420-021-00604-y
26. Xu K, Zhang P, Zhang J, Quan H, Wang J, Liang Y (2021) Identification of potential micro-messenger RNAs (miRNA-mRNA) interaction network of osteosarcoma. Bioengineered 12(1):3275–3293. https://doi.org/10.1080/21655979.2021.1947065
27. Yang S, Wu Y, Xu TH, de Waal PW, He Y, Pu M, Chen Y, DeBruine ZJ, Zhang B, Zaidi SA et al (2018) Crystal structure of the frizzled 4 receptor in a ligand-free state. Nature 560(7720):666–670. https://doi.org/10.1038/s41586-018-0447-x
28. Yang Y, Li H, He Z, Xie D, Ni J, Lin X (2019) MicroRNA-488-3p inhibits proliferation and induces apoptosis by targeting ZBTB2 in esophageal squamous cell carcinoma. J Cell Biochem 120(11):18702–18713. https://doi.org/10.1002/jcb.29178
29. Yu X, Xia J, Cao Y, Tang L, Tang X, Li Z (2021) SNHG1 represses the anti-cancer roles of baicalein in cervical cancer through regulating miR-3127-5p/FZD4/Wnt/beta-catenin signaling. Exp Biol Med (Maywood) 246(1):20–30. https://doi.org/10.1177/1535370220955139
30. Yu X, Yustein JT, Xu J (2021) Research models and mesenchymal/epithelial plasticity of osteosarcoma. Cell Biosci 11(1):94. https://doi.org/10.1186/s13578-021-00600-w
31. Zhang W, Liu T, Li T, Zhao X (2021) Hsa_circRNA_102002 facilitates metastasis of papillary thyroid cancer through regulating miR-488-3p/HAS2 axis. Cancer Gene Ther 28(3–4):279–293. https://doi.org/10.1038/s41417-020-00218-z
32. Zhou X, Jiang J, Guo S (2021) Hsa_circ_0004712 downregulation attenuates ovarian cancer malignant development by targeting the miR-331-3p/FZD4 pathway. J Ovarian Res 14(1):118. https://doi.org/10.1186/s13048-021-00859-0

Publisher's Note